

## Anisotropy of Chemical Transformation from $\text{In}_2\text{Se}_3$ to $\text{CuInSe}_2$ Nanowires through Solid State Reaction

David T. Schoen, Hailin Peng, and Yi Cui\*

*Department of Materials Science and Engineering, Stanford University, Stanford, California 94305-4034*

Received February 11, 2009; E-mail: yicui@stanford.edu

Nanowires (NWs) and other one-dimensional structures have received a great deal of interest related to their applications in many technologies, including nanoelectronics,<sup>1,2</sup> biotechnology,<sup>3</sup> and energy storage<sup>4,5</sup> and conversion.<sup>6–10</sup> Optimizing performance for these applications requires flexibility in materials choice. Great progress has been made in extending existing synthetic techniques, such as the vapor–liquid–solid (VLS)<sup>11</sup> and solution–liquid–solid (SLS)<sup>12</sup> mechanisms for growing NWs, to a large variety of materials,<sup>13,14</sup> but in most cases these techniques are difficult to extend beyond binary compounds, in part because of large contrasts in elemental vapor pressures and activities.<sup>15</sup> Currently there are no general techniques for making high-quality single-crystalline NWs in arbitrary materials systems. One possible approach to obtaining ternary or quaternary NWs is the use of readily available binary NWs as templates to react with compounds containing other desired elements. Although traditional solid-state reaction using micrometer- or larger-sized powders is known to be a brute-force technique for the synthesis of almost any material,<sup>16</sup> it has disadvantages: it requires diffusion over long distance; large strain nucleation barriers must be overcome; and the microstructure of the final materials is difficult to control. However, these disadvantages might be ameliorated or eliminated by using nanocrystalline materials as starting reactants. For example, ZnO NWs have been converted into single-crystalline  $\text{ZnAl}_2\text{O}_4$  spinel nanotubes via solid-state reaction.<sup>17</sup> Single-crystalline colloidal nanocrystals are more chemically active than bulk materials and can readily be transformed into other materials.<sup>18</sup> Se NWs can easily be converted into single-crystalline metal selenide NWs.<sup>19</sup> Here we report the solid-state reaction of single-crystalline  $\text{In}_2\text{Se}_3$  NW templates with Cu at moderate temperatures to form single-crystalline  $\text{CuInSe}_2$  (CIS) NWs and our discovery of a large anisotropy during this chemical transformation.

CIS is a materials system of technological importance and fundamental interest for photovoltaic energy conversion. CIS and the closely related  $\text{Cu}(\text{In,Ga})\text{Se}_2$  (CIGS) materials system hold the record efficiencies ( $\sim 20\%$ ) for thin-film polycrystalline solar cells.<sup>20</sup> Remarkably, the record efficiencies for polycrystalline cells in these systems are higher than those of single-crystalline cells.<sup>21</sup> The underlying reason for this behavior is still in dispute, but it is generally agreed that some structural feature of the active layer prevents interfacial recombination at CIS grain boundaries, by either repelling electrons and holes from the boundaries<sup>21,22</sup> or providing alternative conduction pathways that bypass them.<sup>23</sup> We have previously used CIS NWs to study the interface structure of this system, since their small size allows for characterization by transmission electron microscopy (TEM) without the need for damaging sample-preparation steps.<sup>24</sup> These NWs were grown by the VLS technique; however, the low vapor pressure of Cu compared with In and Se makes the synthesis very sensitive to growth conditions such as temperature and substrate position.

$\alpha$ - $\text{In}_2\text{Se}_3$  ( $\alpha$ -IS) NWs, however, can easily be grown in large quantities by the VLS technique.<sup>25</sup>

The record-efficiency CIGS solar cells are fabricated in a three-step coevaporation process.<sup>26</sup> First, a layer of In, Ga, and Se is deposited at a substrate temperature of 400–450 °C; this is followed by a layer of Cu and Se at a higher temperature of 500–560 °C and then by a capping layer of In, Ga, and Se at the higher temperature. This temperature is sufficient to allow the diffusion of Cu throughout the film and chemically transform it into CIGS. This process has been empirically developed over many years,<sup>20,26,27</sup> and while careful characterization of the final films has been carried out,<sup>28</sup> important information related to chemical and structural transformations inside the films has not been obtained. Nanoscale inhomogeneities in the copper concentration have been proposed as a possible structural feature that might explain the lack of grain boundary recombination;<sup>29</sup> however, there is still little understanding of how such inhomogeneities could form.

In order to explore a route for the facile synthesis of CIS NWs from IS NW templates and also to better understand the process by which CIS is formed by diffusion of Cu into IS, we fabricated structures on 50 nm thick  $\text{SiN}_x$  windows, as shown in Figure 1a. These structures were composed of an IS NW contacted by large Cu pads patterned by electron-beam lithography and evaporation. Since the total thickness of the structure was less than 200 nm, the diffusion of Cu into the NWs could be studied by in situ heating inside the transmission electron microscope.

$\alpha$ -IS is a layered material composed of covalently bonded In and Se within hexagonal sheets (Figure 1b).<sup>30</sup> Neighboring sheets are held together by van der Waals forces. The Se sublattice of the material has an ABAB packing sequence (Figure 1d). One-third of the possible indium sites in the material are vacant and arrange to form a vacant layer. Any additional In vacancies can also order through electrostatic interaction and form a variety of observable repeat distances in IS along the [0001] direction. The largest spacing observed in the [0001] NWs was 0.96 nm, corresponding to the (0002) plane in the bulk unit cell.

IS NWs were previously found to grow in two distinct directions.<sup>25</sup> One growth direction is along [0001], so the NW is composed of IS layers stacked perpendicular to the long axis. The other growth direction is along  $[11\bar{2}0]$ , so the long axis of the NW is parallel to the layers. Because of the vastly different bonding along the long direction of these NWs, one would expect substantially different behaviors, as observed in the case of electrical transport properties.<sup>31</sup> Here we fabricated test structures with NWs of both types, subjected them to temperature cycling at a heating rate of 1 °C/min, and compared the results.

[0001] IS NWs transform to CIS at a very low temperature, near 225 °C. A sequence of electron diffraction (ED) patterns (recorded using the device shown in Figure 2a) acquired during a heating cycle to 350 °C can be seen in Figure 2d–g. Figure 2b,d shows the high-resolution TEM (HRTEM) image and ED pattern, respec-

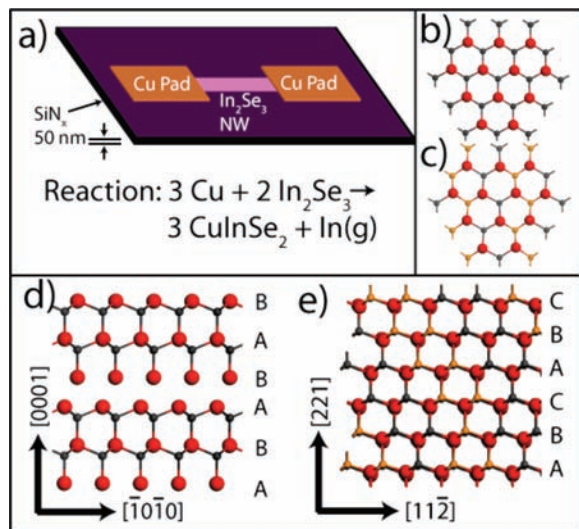


**Figure 1.** (a) Schematic of the test structure and the proposed chemical reaction leading to the transformation. (b) View of the In–Se layers in the IS crystal structure (red, Se; gray, In). (c) View similar to that shown in (b) for a plane of the CIS crystal structure, with orange Cu atoms. (d) [1010] projection of the IS structure showing the ABAB stacking sequence of the Se anion sublattice. (e) [110] projection of the CIS crystal structure showing the ABCABC stacking sequence of the anion sublattice.

tively, for initial IS with the long repeat distance of the (0002) planes. The measured spacings were 9.47 and 1.98 Å for the (0002) and (1120) planes, respectively. At 225 °C, this pattern was observed to briefly smear along this direction and then be replaced by a new pattern with a new repeat distance (Figure 2e). Continued heating revealed a fainter set of spots in locations not observed in the original pattern (Figure 2f). This pattern could be indexed as the CIS structure with measured (112) and (220) spacings of 3.29 and 2.03 Å, respectively, and was preserved upon cooling back to room temperature (Figure 2g). All of the measured spacings matched previous IS and CIS results.<sup>25</sup> The new pattern formed in Figure 2e is dissimilar to that observed for mere superlattice disordering.<sup>25</sup> Real-space images before and after the transformation (Figure 2a,c) revealed no change to the morphology, although a mottled contrast does appear, perhaps due to strain from frustrated longitudinal expansion. There was also a small change in the average NW diameter, which increased upon transformation from 98.9 to 100.1 nm (a change of 1.6%). The NWs retained their single-crystalline structure, which is important for solar cell applications. The 225 °C temperature is significant for IS NWs, as it has been reported that the superlattice reflections observed in ED that arise from ordering of indium vacancies disappear at this temperature.<sup>25</sup> Apparently this chemical disordering is related to the Cu diffusion process, as the CIS ED appeared as soon as the IS superlattice disappeared. The composition of the final phase was verified by energy-dispersive X-ray analysis (EDAX) to have a Cu/In/Se ratio of 1:1:2 within the accuracy of the technique and was uniform through the entire length of the NW [see the Supporting Information (SI)]. No copper gradient, intermediate phases, or untransformed regions were observed, even several micrometers from the copper pads.

In contrast, [1120] NWs did not transform until they were heated to over 580 °C. ED patterns for a heating cycle are shown in Figure 3c–h. Figure 3c shows the initial IS diffraction pattern viewed down the [0001] axis. The main diffraction spots show the underlying hexagonal arrangement, and the faint superlattice peaks indicate the presence of indium ordering relative to the NW surfaces.<sup>25</sup> Once again, at 225 °C the superlattice peaks disappeared, but no other

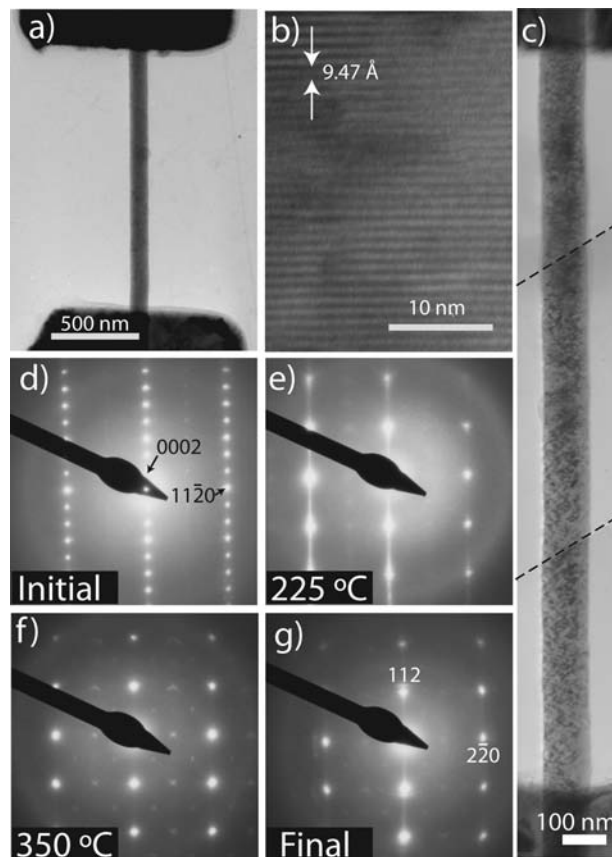


**Figure 2.** (a) Image of an [0001] IS nanowire contacted by two Cu pads (dark contrast at the top and bottom of image). (b) HRTEM image of IS layers. (c) Composite image of the nanowire after the transformation, showing the lack of morphology change. Dotted lines indicate the borders of the constituent images. (d–g) ED patterns of nanowires acquired during a 350 °C temperature cycle. IS zone axis: [1100]. CIS zone axis: [111].

change in the pattern was observed (Figure 3d). The pattern remained unchanged until a temperature of 470 °C, where a variety of new peaks were observed. At a temperature of 585 °C (Figure 3g), the copper electrodes were observed to rapidly disappear, as did the transient peaks observed at 470 °C. When cooled to room temperature, the NWs retained this diffraction pattern (Figure 3h). This pattern could be indexed as CIS viewed in the [221] zone. It is very similar to the IS pattern, as a result of the similarities in the two crystal structures, but the composition was confirmed by EDAX to be near the expected 1:1:2 ratio. A temperature cycle to only 350 °C carried out before the one to 585 °C was insufficient to transform the NWs to CIS. The superlattice peaks disappeared at 225 °C but reappeared upon cooling to room temperature, and only 8% copper was incorporated (see the SI), perhaps indicating the formation of a different CIS phase.

An examination of the crystal structure of CIS and the necessary transformation from IS can shed light on the large anisotropy of the transformation temperatures for the two different growth directions. Given the much smaller size of the cations, one would expect the most energetic part of the transformation to be that required of the anion sublattice. IS has a selenium sublattice in a hexagonal close-packed (HCP) type of arrangement, with hexagonal sheets in an ABAB stacking sequence (Figure 1d). CIS retains hexagonal sheets of selenium, but the packing sequence is more similar to a face-centered cubic (FCC) structure, with an ABCABC stacking sequence (Figure 1e). Normally, the transformation between the HCP and FCC structures requires the creation of a stacking fault, which locally transforms an HCP arrangement to

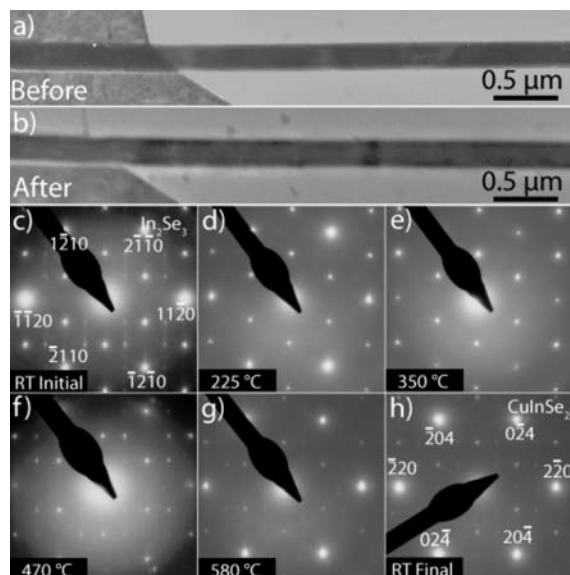


**Figure 3.** (a, b) Low-magnification images of a  $[11\bar{2}0]$  IS NW (a) before and (b) after the transformation, showing the lack of morphology change. (c–h) ED patterns of the nanowire on the  $[0001]$  IS and  $[221]$  CIS zones acquired during a heating cycle to  $585\text{ }^{\circ}\text{C}$ .

an FCC one. In the  $[0001]$  NWs, where the layer structure is perpendicular to the NW long axis, this planar energy is confined only to the NW's cross section, and there is a large amount of free surface to serve as a ready nucleation site for the necessary dislocation loop. Alternatively, it is possible that the entire transformation may be accomplished by a small coordinated shear of the loosely held sheets in the IS structure, which are quickly stabilized by diffusion of copper. For the  $[11\bar{2}0]$  NWs, where the layer structure is parallel to the NW long axis, the transformation can probably be accomplished only by the nucleation and propagation of a dislocation down the entire length of the NW, a process which would be much slower and more energetic. In both cases, the final structure is single-crystalline and apparently free of major defects.

There are two important conclusions to this investigation. First, high-quality single-crystalline CIS can be synthesized by solid-state reaction from IS NW templates. If the initial orientation of the IS NWs can be controlled to lie along the  $[0001]$  direction, this transformation can be accomplished at a very moderate temperature of only  $225\text{ }^{\circ}\text{C}$ , making the process compatible with a variety of substrates. Although this study focused on the transformation of individual NWs, the ultimate production rate and dimension control will be limited only by the ability to produce IS NWs. A 30 min transformation was observed on a  $1\text{ cm}^2$  substrate coated with IS NWs and Cu and produced very little change in the size and morphology of the IS NWs (see the SI).

The second important conclusion is the discovery of a surprising anisotropy in the transition temperature for the transformation of IS to CIS. The effects of orientation on electron- and mass-transport properties is common and unsurprising, but in an NW system, the energetics and mechanism of chemical transformations may vary considerably depending on the orientation of the long axis of the NW relative to the material's crystal structure. This observation

may prove to be an important consideration for the use of NWs in any application involving anisotropic materials and a phase transformation, such as the layered compounds used for lithium intercalation compounds in batteries. It also has implications for CIS solar cell processing: the texture of the IS film grown in the first step of the coevaporation process may play a role in any Cu inhomogeneities in the final CIS film. Controlling this texture may lower the requisite processing temperature, increasing substrate flexibility and reducing the energy cost of fabrication.

**Acknowledgment.** Y.C. acknowledges support from the U.S. Department of Energy under Award DE-FG36-08GOI8004. D.T.S. is an NDSEG and NSF Fellow.

**Supporting Information Available:** Detailed experimental procedures, composition analysis for the NWs in Figures 2 and 3, diffraction patterns from a lower-temperature cycle for the NW in Figure 3, and results from a larger-scale conversion. This material is available free of charge via the Internet at <http://pubs.acs.org>.

## References

- Huang, Y.; Duan, X. F.; Cui, Y.; Lauhon, L. J.; Kim, K. H.; Lieber, C. M. *Science* **2001**, *294*, 1313.
- Bjork, M. T.; Ohlsson, B. J.; Thelander, C.; Persson, A. I.; Deppert, K.; Wallenberg, L. R.; Samuelson, L. *Appl. Phys. Lett.* **2002**, *81*, 4458.
- Cui, Y.; Wei, Q. Q.; Park, H.; Lieber, C. M. *Science* **2001**, *293*, 1289.
- Chan, C.; Peng, H.; Liu, G.; McIlwrath, K.; Zhang, X. F.; Huggins, R. A.; Cui, Y. *Nat. Nanotechnol.* **2008**, *3*, 31.
- Chan, C. K.; Zhang, X. F.; Cui, Y. *Nano Lett.* **2008**, *8*, 307.
- Boukai, A. I.; Bunimovich, Y.; Tahir-Kheli, J.; Yu, J. K.; Goddard, W. A.; Heath, J. R. *Nature* **2008**, *451*, 168.
- Hochbaum, A.; Chen, R. K.; Delgado, R. D.; Liang, W. J.; Garnett, E. C.; Najarian, M.; Majumdar, A.; Yang, P. D. *Nature* **2008**, *451*, 163.
- Huynh, W. U.; Dittmer, J. J.; Alivisatos, A. P. *Science* **2002**, *295*, 2425.
- Wang, X. D.; Song, J. H.; Liu, J.; Wang, Z. L. *Science* **2007**, *316*, 102.
- Tian, B. Z.; Zheng, X. L.; Kempa, T. J.; Fang, Y.; Yu, N. F.; Yu, G. H.; Huang, J. L.; Lieber, C. M. *Nature* **2007**, *449*, 885.
- Morales, A. M.; Lieber, C. M. *Science* **1998**, *279*, 208.
- Trentler, T. J.; Hickman, K. M.; Goel, S. C.; Viano, A. M.; Gibbons, P. C.; Buhro, W. E. *Science* **1995**, *270*, 1791.
- Law, M.; Goldberger, J.; Yang, P. D. *Annu. Rev. Mater. Res.* **2004**, *34*, 83.
- Kuno, M. *Phys. Chem. Chem. Phys.* **2008**, *10*, 620.
- Stull, D. R.; Sinke, G. C. *Thermodynamic Properties of the Elements*; American Chemical Society: Washington, DC, 1956.
- West, A. R. *Basic Solid State Chemistry*; John Wiley & Sons Ltd.: West Sussex, U.K., 1984.
- Fan, H. J.; Knez, M.; Scholz, R.; Nielsch, K.; Pippel, E.; Hesse, D.; Zacharias, M.; Gosele, U. *Nat. Mater.* **2006**, *5*, 627.
- Son, D.; Hughes, S. M.; Yin, Y. D.; Alivisatos, A. P. *Science* **2004**, *306*, 1009.
- Gates, B.; Wu, Y. Y.; Yin, Y. D.; Yang, P. D.; Xia, Y. N. *J. Am. Chem. Soc.* **2001**, *123*, 11500.
- Repins, I.; Contreras, M. A.; Egaas, B.; DeHart, C.; Scharf, J.; Perkins, C. L.; To, B.; Noufi, R. *Prog. Photovoltaics* **2008**, *16*, 235.
- Persson, C.; Zunger, A. *Phys. Rev. Lett.* **2003**, *91*, 266401.
- Zunger, A. *Thin Solid Films* **2007**, *515*, 6160.
- Yan, Y.; Jiang, C. S.; Noufi, R.; Wei, S. H.; Moutinho, H. R.; Al-Jassim, M. M. *Phys. Rev. Lett.* **2007**, *99*, 235504.
- Peng, H.; Xie, C.; Schoen, D. T.; McIlwrath, K.; Zhang, X. F.; Cui, Y. *Nano Lett.* **2007**, *7*, 3734.
- Peng, H.; Schoen, D. T.; Meister, S.; Zhang, X. F.; Cui, Y. *J. Am. Chem. Soc.* **2007**, *129*, 34.
- Contreras, M. A.; Tuttle, J.; Gabor, A.; Tennant, A.; Ramanathan, K.; Asher, S.; Franz, A.; Keane, J.; Wang, L.; Noufi, R. *Sol. Energy Mater. Sol. Cells* **1996**, *41–42*, 231.
- Contreras, M. A.; Egaas, B.; Ramanathan, K.; Hiltner, J.; Swartzlander, A.; Hasoon, F.; Noufi, R. *Prog. Photovoltaics* **1999**, *7*, 311.
- Contreras, M. A.; Romero, M. J.; Noufi, R. *Thin Solid Films* **2006**, *511*, 51.
- Yan, Y.; Noufi, R.; Al-Jassim, M. M. *Phys. Rev. Lett.* **2006**, *96*, 205501.
- Ye, J. P.; Soeda, S.; Nakamura, Y.; Nittono, O. *Jpn. J. Appl. Phys., Part 1* **1998**, *37*, 4264.
- Peng, H.; Xie, C.; Schoen, D. T.; Cui, Y. *Nano Lett.* **2008**, *8*, 1511.

JA901086T